Disturbance observer-based control schemes for quadrotors – a tutorial

Abdurrahman Bayrak & Mehmet Önder Efe

Taylor & Francis
Taylor & Francis Group

Check for updates

Disturbance observer-based control schemes for quadrotors – a tutorial

Abdurrahman Bayrak [a,b] and Mehmet Önder Efe [c]

aGraduate School of Science and Engineering, Hacettepe University, Beytepe, Ankara, Turkey; bUnmanned and Autonomous Systems, System Engineering Department, ASELSAN Inc., Ankara, Turkey; cDepartment of Computer Engineering, Hacettepe University, Beytepe, Ankara, Turkey

ABSTRACT

This paper presents a short tutorial introduction to disturbance observer-based control approaches for the quadrotors. With this tutorial, researchers, engineers and students would be able to implement disturbance observer-based model-in-loop simulations and experiments more easily to design robust autopilot system for the quadrotors. To achieve this, first of all, the modeling and controlling of a quadrotor are explained and all linear disturbance observer-based control approaches in the literature are adapted in its overall nonlinear architecture. Disturbance observer-based control design steps are given in detail by design challenges. To show their disturbance rejection capabilities and practical applicability, two flight simulation scenarios are carried out. For all simulation cases, we only take into account the external disturbances in rotational motions. While we give the attitude trajectory commands to quadrotor attitude control architecture in the first scenario, we issue both way-point and trajectory commands to an outer loop controlling the translational motions in the second one. Presented disturbance observer-based control approaches have successfully completed the given reference commands in the presence of the external disturbances even under the measurement noise. Moreover, simulation experiments have shown that UDEBC approach transmits the external disturbance and measurement noise effects to the actuators directly. As a result, for UDEBC approach, it should be kept in mind that flight accidents may occur due to excessive ESC heating. Baseline attitude controller without disturbance observer-based control approach have failed to follow the given reference commands. The simulation studies have also proved the practical applicability of these methods, which are successful even under measurement noise.

1. Introduction

Quadrotors have been widely used for many different civilian and military purposes thanks to their low cost, agile maneuverability, Vertical Takeoff and Landing (VTOL) property, small size and hover capability. In recent years, the fact that many people prefer rotary wing unmanned aerial vehicles in many areas such as photography, search and rescue,

CONTACT Abdurrahman Bayrak ✉ abayrak26@gmail.com

emergency response and swarm applications shows that the control of the quadrotors is still among the hot topics. Nonlinear, multi-variable, coupled and under-actuated dynamics of the quadrotors make modeling and control of them a challenging design problem. Furthermore, uncertainty and unavoidable external disturbances such as wind, unmodeled dynamics, neglected aerodynamic effects, variable weight suspended payloads, measurement and input noise make controller design even more difficult. While wind and variable weight suspended payloads are the environmental factors, unmodeled dynamics and measurement noise are caused by the modeling errors and available sensors, respectively. Some of these unknown factors are the matched external disturbances as they effect the control input signal for the rotational motion of the quadrotor. For better understanding, while the effect of wind on rotational movement of a quadrotor is considered as matched disturbance, the effect of wind on translational movement of a quadrotor is considered as unmatched disturbance. The rejection of unmatched disturbances is the out of scope for this paper. Disturbance resistant control systems generally reject the disturbances up to a certain limit. Therefore, bounded matched external disturbances will be considered.

In the literature, numerous studies focus on the control of the quadrotors (Nascimento and Saska 2019). The most common controller structure is the Proportional Integral Derivative (PID) control which is widely used in commercial quadrotors (Bouabdallah, Noth, and Siegwart 2004; Bouabdallah 2007; Salih et al. 2010; Khatoon, Shahid, and Chaudhary 2014). The other common control structures in the literature include both linear and nonlinear controllers: Linear Quadratic Regulator (LQR), Model Predictive Control (MPC), Back-Stepping Control (BSC), Sliding Mode Control (SMC), H-infinity Control and Geometric Control (GC) (Rinaldi, Chiesa, and Quagliotti 2014; Reyes-Valeria et al. 2013; Bangura and Mahony 2014; Alexis, Nikolakopoulo, and Tzes 2012; Chen, F. et al. 2016; Madani and Benallegue 2006; Bouabdallah and Siegwart 2005, 2007; Zulu and John 2016; Shaik and Whidborne 2016; Ortiz, Minchala, and Reinoso 2016; Shi, Zhang, and Zhou 2015).

Nascimento and Saska (2019) have presented an exhaustive review of recent advances for position, altitude and attitude control of multi-rotor aerial vehicles from linear to non-linear control approaches. Readers can refer to their work for a range of multi-rotor aerial vehicle control approaches such as intelligent control, robust control, adaptive control, fractional order control, data-driven control, disturbance observer-based control (DOBC), active disturbance rejection control (ADRC) and more. Among these control approaches, the ADRC and DOBC have recently gained popularity not only in the control of quadrotors but also in the control of most industrial mechanical systems including external disturbances and unknown dynamics which are widely encountered in most control problems. Especially for practical applications, the ADRC and DOBC approaches emerge as robust control methods given the complexity of quadrotor control as well as unknown external disturbances and uncertainties. The ADRC approach is also known as extended state observer (ESO). Tracking differentiator, ESO and state error feedback control law are the main parts to design an ADRC approach. Zhang et al. (2018) have proposed a new double closed-loop ADRC approach for the quadrotors.

An another powerful robust control method is disturbance observer-based control approach and it has two Degrees of Freedom (2-DoF) structure (Chen, W. et al. 2016; Castillo et al. 2019; Bayrak and Efe 2021). DOBC approaches add an inner loop estimating and rejecting the external disturbances to baseline controller. As a consequence,

both robustness and performance requirements for DOBC approaches are simultaneously achieved, while for conventional controllers there is a trade-off between robustness and performance.

In the study of Chen, W. et al. (2016), an overview about the DOBC and related approaches in the literature is presented. Castillo et al. (2019) propose a novel quaternion-based DOB attitude controller structure for aggressive maneuvering and strong disturbances such as suspended payloads. In this paper, for the quadrotors, we discuss all linear DOBC approaches found in the literature, namely, we study Conventional Disturbance Observer-Based Control (CDOBC) (Tamaki et al. 1986; Wang and Chen 2016; Bayrak and Efe 2019), Equivalent Input Disturbance-Based Control (EIDBC) (She et al. 2008; She, Xin, and Pan 2011; Cai et al. 2019), Uncertainty Disturbance Estimator-Based Control (UDEBC) (Zhong and Rees 2004; Zhong, Kuperman, and Stobart 2011; Sanz et al. 2016a, 2016b), Time Domain Disturbance Observer-Based Control (TDDOBC) (Yang, Chen, and Li 2010; Lazim et al. 2019) and Output Error Based Disturbance Observer-Based Control (OEBDOBC) (Kürkçü, Kasnakoğlu, and Efe 2018). In our previous study (Bayrak and Efe 2021), we have presented a comprehensive comparison of these disturbance observer-based robust control approaches by considering the advantages and disadvantage of each method such as time delay and measurement noise sensitivity, and derived the robustness and performance equations providing useful insights for choosing the best DOBC approach.

The origin of DOBC approach is presented in the work of Tamaki et al. (1986), and it has been a source of inspiration for researchers in the development of other DOBC approaches. Bayrak and Efe (2019) have used the CDOBC approach to reject external disturbances caused by wind in the rotational motion of a quadrotor. To further improve the trajectory tracking precision of a quadrotor, a Linear Dual DOBC scheme is proposed by Wang and Chen (2016) with the modification of the CDOBC approach. In the studies of She et al. (2008) and She, Xin, and Pan (2011), a new disturbance rejection scheme named as EIDBC is proposed and applied to Dual-Stage Feed Drive Control System. A new disturbance suppression scheme that is sliding mode observer-based EID approach for the under-actuated subsystem of a quadrotor is presented in the work of Cai et al. (2019). The works of Zhong and Rees (2004) and Zhong, Kuperman, and Stobart (2011) are the studies that are accepted as fundamental of UDEBC architecture. Sanz et al. (2016a) have proposed a UDE-based robust control method that is validated in real-time applications for the attitude and the altitude control of quadrotors. Sanz et al. (2016b) in another work have proposed a modified UDE control approach and have validated it with real-time quadrotor experiments. They have obtained much better performance even under the presence of large time delays. TDDOBC approach was first presented in the study of Yang, Chen, and Li (2010) with the robust autopilot design problem for a missile system affected by disturbances and uncertainties, and it is applied to quadrotors by proposing a robust disturbance observer-based feedback linearization approach to eliminate adverse effects to the formation flight of multiple quadrotors (Lazim et al. 2019). Kürkçü, Kasnakoğlu, and Efe (2018) have proposed the novel DOBC approach that removes the need for the inverse of the nominal system in CDOBC approach and is more suitable than CDOBC approach for non-minimum phase systems.

Mathematical modeling of the quadrotors is another challenging area due to considered aerodynamic effects, actuator and sensor dynamics. So far, different data-driven methods

using experimental input output data and allowing tuning of the controller parameters have often been used (Invernizzi et al. 2016). These methods allow us fast deployment of the control system besides an accurate modeling of the system. As some DOBC approaches require priory knowledge of nominal plant or inverse of nominal plant, the merging data-driven methods and DOBC structures emerge as an open field that needs to be studied. Treesatayapun and Munoz-Vazquez (2021) have obtained data-driven model by means of fuzzy rules emulating a neural network and proposed a discrete time disturbance observer improving closed loop performance with an output feedback controller considering input output information.

In this paper, we present a short tutorial introduction to DOBC approaches for attitude control of the quadrotors by applying five different linear DOBC methods. We also analyze disturbance suppression capabilities of them in detail by discussing design challenges and practical applicability. A nonlinear controller that is designed by taking into account nonlinear quadrotor dynamics namely BSC is used in all simulation studies. Whether a linear or nonlinear controller is preferred, it has been confirmed by simulation studies that when the DOBC structures presented here are integrated into the general quadrotor control system, the system becomes more robust. With this tutorial, researchers, engineers and students would be able to implement disturbance observer-based model-in-loop simulations and experiments more easily to design robust autopilot system for the quadrotors.

The remainder of this paper is organized as follows. Section 2 handles the control architectures of quadrotor and DOBC approaches in detail. The next section includes simulation experiments to discuss the disturbance rejection performances and practical applicability of DOBC structures given in this paper. Finally, concluding remarks are presented.

2. Methodology

2.1. Mathematical model of a quadrotor

This section presents the mathematical equations required for a quadrotor unmanned aerial vehicle control. We select the quadrotor model as in Figure 1.
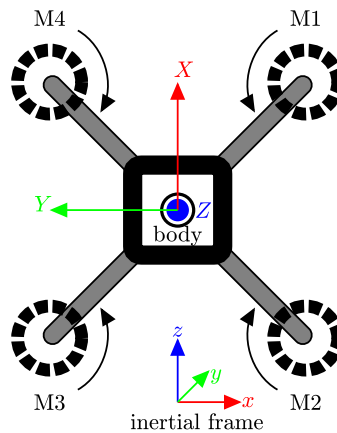

Figure 1. The quadrotor model in cross configuration (ENU frame).

$$\begin{bmatrix} m\ddot{x} \\ m\ddot{y} \\ m\ddot{z} \end{bmatrix} = \begin{bmatrix} (c_\psi s_\theta c_\phi + s_\psi s_\phi)U_z + d_x \\ (s_\psi s_\theta c_\phi - c_\psi s_\phi)U_z + d_y \\ (c_\theta c_\phi)U_z - mg + d_z \end{bmatrix} \tag{1}$$

$$\begin{bmatrix} I_x\dot{p} \\ I_y\dot{q} \\ I_z\dot{r} \end{bmatrix} = \begin{bmatrix} (U_\phi + (I_y - I_z)qr - Jq\Omega_S) + d_\phi \\ (U_\theta + (I_z - I_x)pr + Jp\Omega_S) + d_\theta \\ (U_\psi + (I_x - I_y)pq) + d_\psi \end{bmatrix} \tag{2}$$

Equations (1) and (2) are the translational and rotational dynamics of a quadrotor, respectively, where $c : cos$ and $s : sin$, x, y, z are the relative position of a quadrotor in the inertial frame, ϕ, θ, ψ are the Euler angles, p, q, r are the body angular rates, m is the quadrotor mass, I is the quadrotor body diagonal inertia matrix, g is the gravity acceleration, U_z is the total lift control force input, U_ϕ, U_θ, U_ψ are the torque control inputs, J is the propeller moment inertia value, d_x, d_y are the bounded unknown mismatched external disturbances, $d_z, d_\phi, d_\theta, d_\psi$ are the bounded unknown matched external disturbances, and finally Ω_S is $\Omega_2 + \Omega_4 - \Omega_1 - \Omega_3$. Ω_i is the ith motor speed. Equation (3) shows the conversion from the body angular rates to the Euler angle rates.

$$\begin{bmatrix} \dot{\phi} \\ \dot{\theta} \\ \dot{\psi} \end{bmatrix} = \begin{bmatrix} 1 & s_\phi t_\theta & c_\phi t_\theta \\ 0 & c_\phi & -s_\phi \\ 0 & \dfrac{s_\phi}{c_\theta} & \dfrac{c_\phi}{c_\theta} \end{bmatrix} \begin{bmatrix} p \\ q \\ r \end{bmatrix} \tag{3}$$

Equation (4) shows the rotation matrix from body to inertial frame.

$$\mathbf{R} = \begin{bmatrix} c_\psi c_\theta & c_\psi s_\theta s_\phi - s_\psi c_\phi & c_\psi s_\theta c_\phi + s_\psi s_\phi \\ s_\psi c_\theta & s_\psi s_\theta s_\phi + c_\psi c_\phi & s_\psi s_\theta c_\phi - c_\psi s_\phi \\ -s_\theta & c_\theta s_\phi & c_\theta c_\phi \end{bmatrix} \tag{4}$$

We can write the following control input equations by using the quadrotor model in Figure 1.

$$\mathbf{U} = \begin{bmatrix} U_z \\ U_\phi \\ U_\theta \\ U_\psi \end{bmatrix} = \begin{bmatrix} 1 & 1 & 1 & 1 \\ -\dfrac{l}{\sqrt{2}} & -\dfrac{l}{\sqrt{2}} & \dfrac{l}{\sqrt{2}} & \dfrac{l}{\sqrt{2}} \\ -\dfrac{l}{\sqrt{2}} & \dfrac{l}{\sqrt{2}} & \dfrac{l}{\sqrt{2}} & -\dfrac{l}{\sqrt{2}} \\ -\kappa & \kappa & -\kappa & \kappa \end{bmatrix} \begin{bmatrix} f_1 \\ f_2 \\ f_3 \\ f_4 \end{bmatrix} \tag{5}$$

$$\begin{bmatrix} \Omega_1^2 \\ \Omega_2^2 \\ \Omega_3^2 \\ \Omega_4^2 \end{bmatrix} = \begin{bmatrix} \dfrac{1}{4K_F} & -\dfrac{\sqrt{2}}{4K_Fl} & -\dfrac{\sqrt{2}}{4K_Fl} & -\dfrac{1}{4\kappa K_F} \\ \dfrac{1}{4K_F} & -\dfrac{\sqrt{2}}{4K_Fl} & \dfrac{\sqrt{2}}{4K_Fl} & \dfrac{1}{4\kappa K_F} \\ \dfrac{1}{4K_F} & \dfrac{\sqrt{2}}{4K_Fl} & \dfrac{\sqrt{2}}{4K_Fl} & -\dfrac{1}{4\kappa K_F} \\ \dfrac{1}{4K_F} & \dfrac{\sqrt{2}}{4K_Fl} & -\dfrac{\sqrt{2}}{4K_Fl} & \dfrac{1}{4\kappa K_F} \end{bmatrix} \begin{bmatrix} U_1 \\ U_2 \\ U_3 \\ U_4 \end{bmatrix} \tag{6}$$

where $\mathbf{U}$ is the control signal, $\Omega = [\Omega_1 \; \Omega_2 \; \Omega_3 \; \Omega_4]^T$ is the actual rotor speed in rad/sec, f_i is the thrust value generated by each rotor, l is the arm length of the quadrotor, and κ is the conversion factor between the thrust and the torque values. $\tau_i = \kappa f_i$. τ_i is the torque value generated by each rotor. $f_i = K_F \Omega_i^2$. K_F is the positive motor thrust factor. We use the below first-order transfer function as a rotor dynamics model.

$$\frac{\Omega_i(s)}{\Omega_{di}(s)} = \frac{1}{T_{rot}s + 1} \tag{7}$$

where T_{rot} is the time constant of the rotor dynamics and $\Omega_{\mathbf{d}} = [\Omega_{d1} \; \Omega_{d2} \; \Omega_{d3} \; \Omega_{d4}]^T$ is the desired rotor speed in rad/sec.

2.2. Robust control schemes for the quadrotors

In this section, we present in detail five disturbance observer-based control schemes for the quadrotors, three in frequency domain and two in time domain. Let $\mathbf{r_d} = [z_d \; \phi_d \; \theta_d \; \psi_d]^T$ denote the reference signals for altitude and attitude behaviors. Let $\mathbf{y_r} = [z \; \phi \; \theta \; \psi]^T$ denote the actual altitude and attitude states. $\mathbf{d}$, $\mathbf{n}$ and $\hat{\mathbf{d}}$ are the external disturbance input, measurement noise input and estimation of the lumped disturbances, respectively. Reference signal tracking error $\mathbf{e}$ is as follows:

$$\mathbf{e} = \mathbf{r_d} - \mathbf{y_r} \tag{8}$$

In the given DOBC block diagrams in the next sections, "Att&Altitude Controller" block is the baseline controller. "Plant" block is the nonlinear equations of the quadrotor and contains Equations (1)–(4). While "Force&Torques to Speed" block is the square root of Equation (6), "Speed to Force&Torques" block includes Equation (5). Finally, "Actuator Dynamics" block includes Equation (7) for each rotor. Altitude variables for DOE parts of the approaches presented in this paper are taken zero as we take into account the external disturbances in attitude behavior of the quadrotor.

2.2.1. Conventional disturbance observer based control (CDOBC) scheme
Figure 2 shows the overall attitude and altitude control scheme using CDOBC approach for the quadrotors. As shown in Figure 2, DOE structure consists of a combination of the inverse of nominal plant and $\mathbf{Q(s)}$ low pass filter. LPF design directly effects the disturbance rejection capability of the overall system. To achieve a good disturbance rejection performance in the attitude control of the quadrotors, we recommend designing $\mathbf{Q(s)}$ LPF by following the steps below instead of first-order LPF.

(1) Develop a simple and fast Proportional-Derivative (PD) controller under the unit step reference input function for the nominal plant of the quadrotor.
(2) Take overall closed loop system as $\mathbf{Q(s)}$ LPF.

To find the inverse of nominal plant and design a $\mathbf{Q(s)}$ LPF, we obtain the following nominal plant of the quadrotor after the linearization process of nonlinear quadrotor
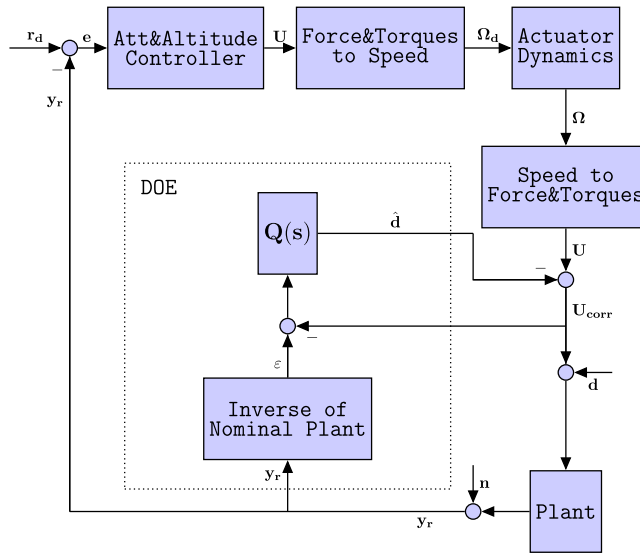
Figure 2. CDOBC scheme for the quadrotors.

dynamics.

$$\begin{bmatrix} \ddot{z} \ \ddot{\phi} \ \ddot{\theta} \ \ddot{\psi} \end{bmatrix}^T = \begin{bmatrix} 0 & \frac{1}{I_x s^2} & \frac{1}{I_y s^2} & \frac{1}{I_z s^2} \end{bmatrix}^T \tag{9}$$

As a consequence, "Inverse of Nominal Plant" block generates the following output:

$$\varepsilon = \text{diag}(0, I_x s^2, I_y s^2, I_z s^2)\mathbf{y_r} \tag{10}$$

"$\mathbf{Q(s)}$" block is found as follows from the above LPF design steps.

$$\mathbf{Q(s)} = \text{diag}\left(0, \frac{\frac{K_d}{I_x}s + \frac{K_p}{I_x}}{s^2 + \frac{K_d}{I_x}s + \frac{K_p}{I_x}}, \right.$$
$$\left. \frac{\frac{K_d}{I_y}s + \frac{K_p}{I_y}}{s^2 + \frac{K_d}{I_y}s + \frac{K_p}{I_y}}, \frac{\frac{K_d}{I_z}s + \frac{K_p}{I_z}}{s^2 + \frac{K_d}{I_z}s + \frac{K_p}{I_z}} \right) \tag{11}$$

where K_p and K_d are the PD controller parameters for LPF design.

2.2.2. Output error- based disturbance observer- based control (OEBDOBC) scheme

Figure 3 shows the overall control structure based on the output error-based disturbance observer estimator presented in the study of Kürkçü, Kasnakoğlu, and Efe (2018). Their DOE structure is adapted for the quadrotors. In DOE structure, "Nominal Plant" block includes (9). "$\mathbf{K_{obs}}$" block has a simple PD control structure obtained for the nominal plant (9) under the unit step reference input function (LPF design step 1). The following
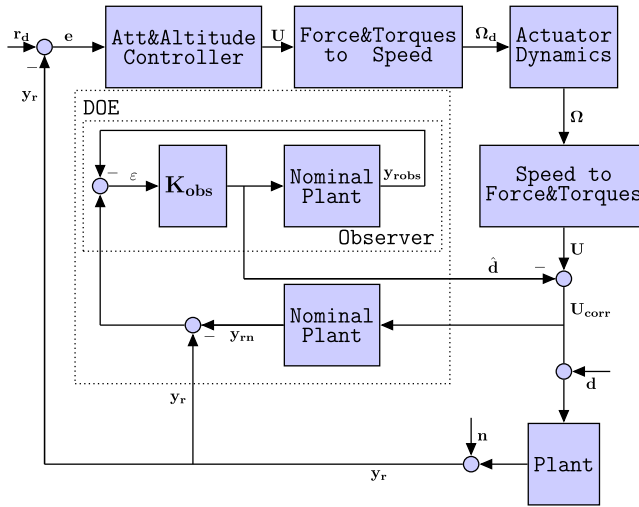
Figure 3. OEBDOBC scheme for the quadrotors.

equation can be written for the observer part.

$$\varepsilon = \mathbf{y_r} - \mathbf{y_{rn}} - \mathbf{y_{robs}} \tag{12}$$

where $\mathbf{y_{rn}} = [0 \ \phi_n \ \theta_n \ \psi_n]^T$ is the nominal output of the quadrotor and $\mathbf{y_{robs}} = [0 \ \phi_{obs} \ \theta_{obs} \ \psi_{obs}]^T$ is the output of observer part.

2.2.3. Equivalent input disturbance- based control (EIDBC) scheme

Figure 4 illustrates the equivalent input disturbance-based control structure. We adapt it from the work of She et al. (2008) for the quadrotors. EIDBC scheme requires a state observer design part and LPF design part independently.

State observer design block diagram is demonstrated in Figure 5. It includes the following equation and "$\mathbf{B}_i^+$" block.

$$\dot{\hat{\mathbf{x}}}(t) = \mathbf{A_{n}}_i\hat{\mathbf{x}}_i(t) + \mathbf{B_{n}}_i U_i(t) + \mathbf{L}_i[y_{ri}(t) - \hat{y}_i(t)] \tag{13}$$

$$\mathbf{B}_i^+ = (\mathbf{B_{n}}_i^T \mathbf{B_{n}}_i)^{-1}(\mathbf{B_{n}}_i^T \mathbf{L}_i) \tag{14}$$

where $i \in (\phi, \theta, \psi)$, $\hat{\mathbf{x}}_i(t)$ and $\hat{y}_i(t) = \mathbf{C_{n}}_i\hat{\mathbf{x}}_i(t)$ are the observer plant state and its output, respectively. $\mathbf{L}_i$ is the observer gain. $\mathbf{A_{n}}_i$, $\mathbf{B_{n}}_i$ and $\mathbf{C_{n}}_i$ matrices are system matrix, control matrix and output matrix of nominal plant in controllable canonical form, respectively. U_i is control signal for roll, pitch and yaw movements. ($\mathbf{A_{n}}_i \in \Re^{2\times2}$, $\mathbf{B_{n}}_i \in \Re^{2\times1}$, $\mathbf{C_{n}}_i \in \Re^{1\times2}$, $\mathbf{L}_i \in \Re^{2\times1}$, $\mathbf{B_i^+} \in \Re^{1\times2}$, $\hat{\mathbf{x}}_i \in \Re^{2\times1}$, $\hat{y}_i \in \Re^{1\times1}$) LPF "$\mathbf{F(s)}$" is chosen as follows:

$$\mathbf{F(s)} = \text{diag}\left(0, \frac{T_e}{s + T_e}, \frac{T_e}{s + T_e}, \frac{T_e}{s + T_e}\right) \tag{15}$$
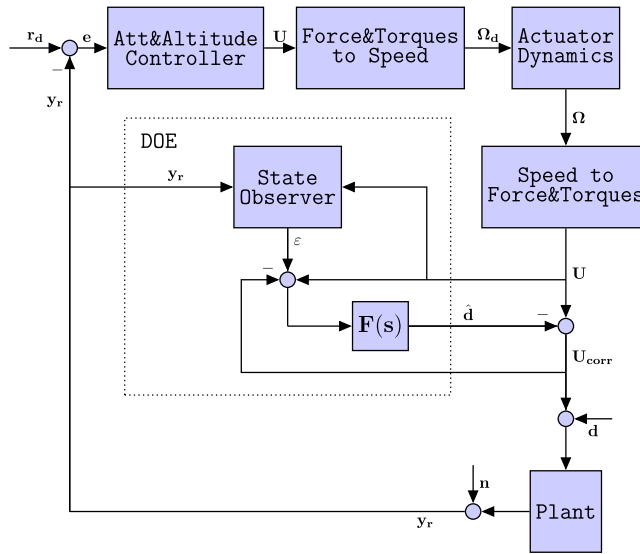
where T_e is the LPF cutoff frequency.

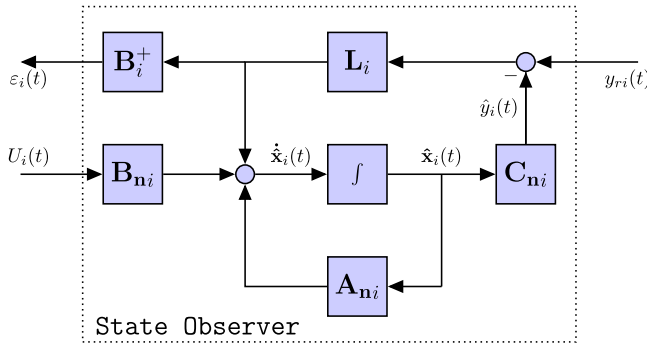**Figure 4.** EID scheme for the quadrotors.

Figure 5. State Observer block diagram in EID scheme.

2.2.4. Time domain disturbance observer- based control (TDDOBC) scheme

Time domain disturbance observer-based control scheme is presented in Figure 6 (Yang, Chen, and Li 2010). Figure 7 shows Disturbance Observer block diagram in DOE part of it. Disturbance Observer design introduces the following dynamics:

$$\hat{d}_i = v_i(t) + \mathbf{L}_i \tilde{\mathbf{x}}_i(t) \tag{16}$$

$$\dot{v}_i(t) = -\mathbf{L}_i \mathbf{B}_{\mathbf{n}i}(v_i(t) + \mathbf{L}_i \tilde{\mathbf{x}}_i(t)) - \mathbf{L}_i(\mathbf{A}_{\mathbf{n}i} \tilde{\mathbf{x}}_i(t) + \mathbf{B}_{\mathbf{n}i} U_{corri}(t)) \tag{17}$$

$$\tilde{\mathbf{x}}_i(t) = \left[y_{ri}(t) \ \dot{y}_{ri}(t) \right]^T \tag{18}$$

where $i \in (\phi, \theta, \psi)$, $\tilde{\mathbf{x}}_i(t)$ is the disturbance observer plant state. $\mathbf{L}_i$ is the observer gain. $\mathbf{A}_{\mathbf{n}i}$, $\mathbf{B}_{\mathbf{n}i}$ and $\mathbf{C}_{\mathbf{n}i}$ matrices are system matrix, control matrix and output matrix of nominal plant in observable canonical form, respectively. U_{corri} is corrected control signal for roll, pitch and yaw movements ($\mathbf{A}_{\mathbf{n}i} \in \mathfrak{R}^{2\times2}$, $\mathbf{B}_{\mathbf{n}i} \in \mathfrak{R}^{2\times1}$, $\mathbf{C}_{\mathbf{n}i} \in \mathfrak{R}^{1\times2}$, $\mathbf{L}_i \in \mathfrak{R}^{1\times2}$, $\tilde{\mathbf{x}}_i \in \mathfrak{R}^{2\times1}$).
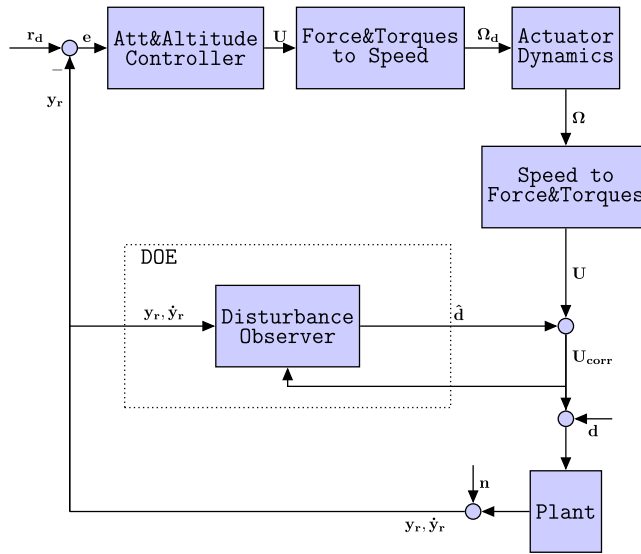
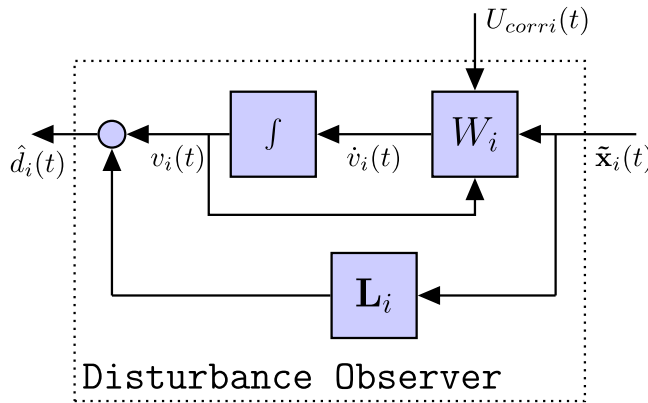**Figure 6.** TDDOBC scheme for the quadrotors.

Figure 7. Disturbance Observer block diagram in TDDOBC scheme.

2.2.5. Uncertainty disturbance estimator- based control (UDEBC) scheme

Figure 8 demonstrates the uncertainty and disturbance estimator-based control scheme (Zhong and Rees 2004). The main idea for designing a UDE-based controller for the quadrotors is to obtain coupled dynamics from decoupled dynamics of the quadrotors, and to treat their nonlinear terms as uncertainty and disturbance. As a consequence, when we follow the procedures in the study of Sanz et al. (2016a), we obtain the following UDE controller rule by simplifying the equations.

$$U_i = I_i \left(\left(K_i + \frac{1}{T_i} \right) e_s + \frac{K_i}{T_i} \int e_{si} + \lambda_i \dot{e}_{si} + \ddot{r}_{di} \right) \tag{19}$$

where $i \in (\phi, \theta, \psi)$, $[I_\phi \ I_\theta \ I_\psi] = [I_x \ I_y \ I_z]$ and $e_{si} = \lambda_i e_i + \dot{e}_i$. K_i, T_i, λ_i are the UDE controller parameters. T_i determines the required low pass filter cutoff frequency for the
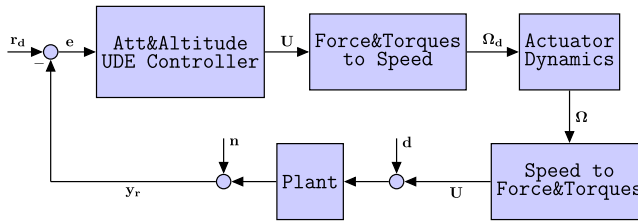
Figure 8. UDEBC scheme for the quadrotors.

uncertainty and disturbance estimation. UDE controller rule includes the low pass filter $G_f = 1/(Ts + 1)$.

2.2.6. Baseline controller design

As linear controllers such as PID and LQR are obtained for the simplified model of the quadrotors, strong disturbances are poorly rejected (Bouabdallah and Siegwart 2007). However, even if there is a controller with the worst performance in disturbance rejection, DOBC approaches with 2-DoF structures remove this disadvantage and add strong robustness against disturbances and uncertainties. We chose the BSC approach which has better disturbance rejection capability than linear controllers as baseline attitude and altitude control to take into account all the nonlinear dynamics of the quadrotor. When we execute the rules presented in the work of Madani and Benallegue (2006), we obtain the following BS control signals:

$$U_z = \frac{m}{\cos(\phi)\cos(\theta)}(\ddot{r}_{dz} + e_z + g - \alpha_{z1}(e_{bz} + \alpha_{z1} * e_z) - \alpha_{z2}e_{bz}) \qquad (20)$$

where α_{z1}, α_{z2} are the BS controller parameters for altitude control, $e_z = r_{dz} - y_{rz}$ and $e_{bz} = \dot{y}_{rz} - \dot{r}_{dz} - \alpha_{z1}e_z$.

$$U_\phi = I_x(\ddot{r}_{d\phi} + e_\phi - a_1\dot{\theta}\dot{\psi} - a_2\dot{\theta}\Omega_S - \alpha_{\phi1}(e_{b\phi} + \alpha_{\phi1}e_\phi) - \alpha_{\phi2}e_{b\phi}) \qquad (21)$$

where $\alpha_{\phi1}, \alpha_{\phi2}$ are the BS controller parameters for roll angle control, $e_\phi = r_{d\phi} - y_{r\phi}$, $e_{b\phi} = \dot{y}_{r\phi} - \dot{r}_{d\phi} - \alpha_{\phi1}e_\phi$, $a_1 = (I_y - I_z)/I_x$ and $a_2 = -J/I_x$.

$$U_\theta = I_y(\ddot{r}_{d\theta} + e_\theta - a_3\dot{\phi}\dot{\psi} - a_4\dot{\phi}\Omega_S - \alpha_{\theta1}(e_{b\theta} + \alpha_{\theta1}e_\theta) - \alpha_{\theta2}e_{b\theta}) \qquad (22)$$

where $\alpha_{\theta1}, \alpha_{\theta2}$ are the BS controller parameters for pitch angle control, $e_\theta = r_{d\theta} - y_{r\theta}$, $e_{b\theta} = \dot{y}_{r\theta} - \dot{r}_{d\theta} - \alpha_{\theta1}e_\theta$, $a_3 = (I_z - I_x)/I_y$ and $a_4 = J/I_y$.

$$U_\psi = I_z(\ddot{r}_{d\psi} + e_\psi - a_5\dot{\theta}\dot{\phi} - \alpha_{\psi1}(e_{b\psi} + \alpha_{\psi1}e_\psi) - \alpha_{\psi2}e_{b\psi}) \qquad (23)$$

where $\alpha_{\psi1}, \alpha_{\psi2}$ are the BS controller parameters for yaw angle control, $e_\psi = r_{d\psi} - y_{r\psi}$, $e_{b\psi} = \dot{y}_{r\psi} - \dot{r}_{d\psi} - \alpha_{\psi1}e_\psi$ and $a_5 = (I_x - I_y)/I_z$.

3. Simulation experiments

3.1. Simulation results

In this section, two flight simulation scenarios are considered to verify the presented disturbance observer schemes. The goal of the first scenario is to show that external
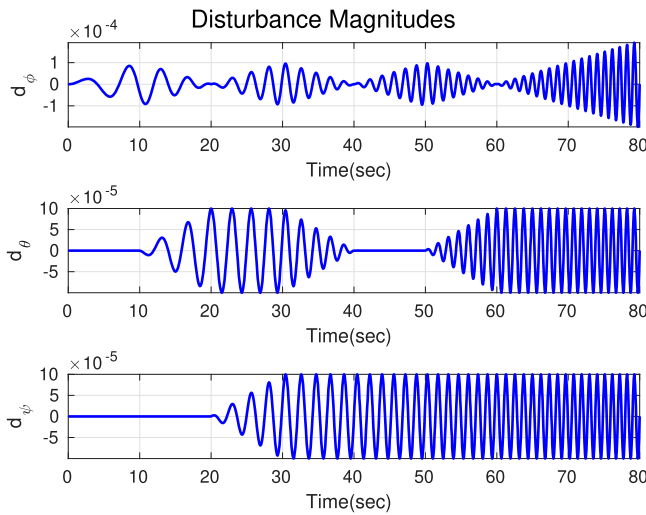
Figure 9. Magnitudes of external disturbances for rotational motion of Crazyflie 2.0.
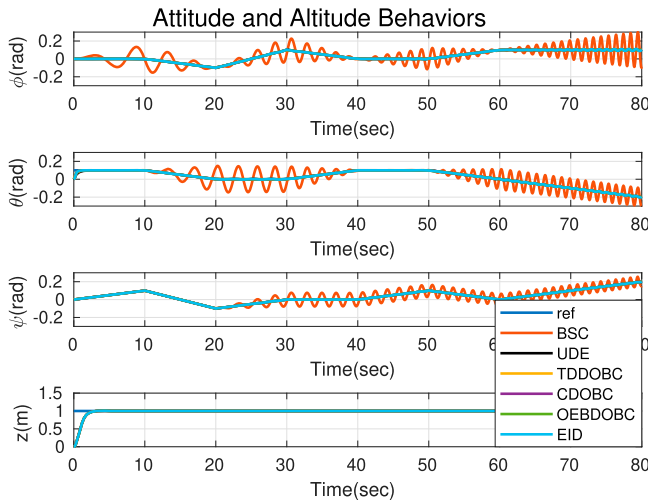

Figure 10. Attitude and altitude behaviors of the quadrotor.

disturbances $(d_\phi, d_\theta, d_\psi)$ in the rotational dynamics of the quadrotor are rejected under the attitude trajectory commands while the altitude is maintained at a constant value. In the second scenario, we aim to demonstrate the practical applicability of the disturbance observer-based control approaches under the certain reference way-point and trajectory commands. All simulation parameters are given in the appendix section.

For the first scenario, we selected the magnitudes of the external disturbances in the rotational dynamics as shown in Figure 9 and applied them to the quadrotor for 80 seconds under the given roll, pitch and yaw reference signals. Figure 10 presents the attitude and altitude behaviors of the quadrotor. Under a constant altitude reference value, while all DOBC approaches rejected the applied external disturbances, BSC approach could not perform the same disturbance rejection performance. When we zoom in the roll behavior
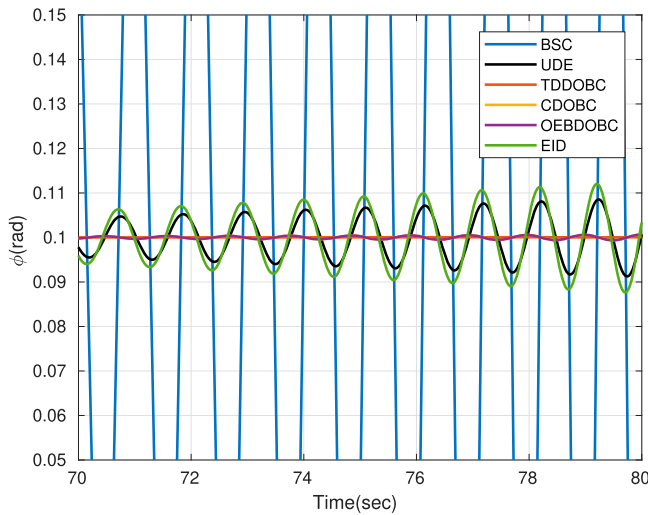
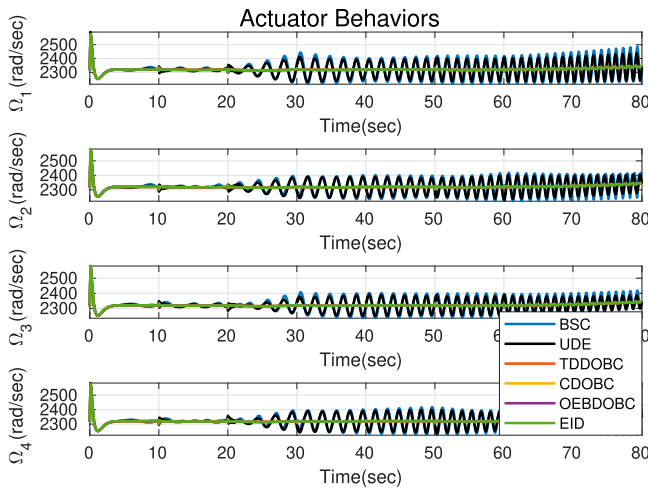**Figure 11.** Roll behavior of the quadrotor (zoomed in).

Figure 12. Actuator behaviors of the quadrotor.

of the quadrotor in Figure 11, it can be seen that EIDBC and UDEBC approaches have worse disturbance rejection performance than other DOBC approaches. It should be kept in mind that disturbance suppression performances of EIDBC and UDEBC approaches can be improved after adjusting the parameters like bandwidth parameters in the DOE structures. For our simulation studies, their rejection performances are within acceptable limits without any adjusting. Figure 12 illustrates the actuator behaviors of the quadrotor under the disturbance. From Figure 12, we can see that BSC and UDEBC transmit the external disturbance effects to the actuators. These actuator oscillations in the BSC and UDEBC approaches cause actuator ESCs to overheat in case of continuous exposure to external disturbances. It should not be forgotten that flight accidents may occur as a result.

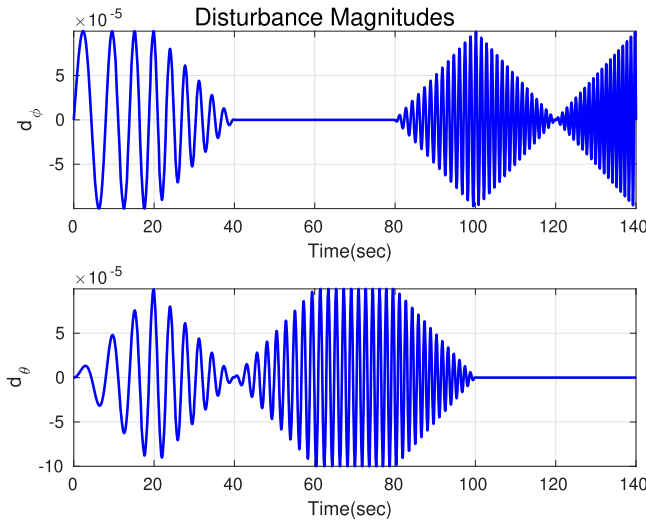**Figure 13.** Position controller block for the quadrotors.

Figure 14. Magnitudes of external disturbances for way-point and trajectory tracking of Crazyflie 2.0.

For the second scenario, we added an outer loop controlling translational motions to attitude control mechanism in Figure 13 and issued both the reference way-point and trajectory commands after setting the magnitudes of the external disturbances in the rotational dynamics as shown in Figure 14. Position block control rule in Figure 13 includes Equations (24)–(25) and (26).

$$\begin{bmatrix} \phi_d \\ \theta_d \end{bmatrix} = \begin{bmatrix} \dfrac{c(\theta)c(\phi)}{g}(s(\psi)\dot{x}_p - c(\psi)\dot{y}_p) \\ \dfrac{c(\theta)c(\phi)}{g}(c(\psi)\dot{x}_p + s(\psi)\dot{y}_p) \end{bmatrix} \tag{24}$$

$$\begin{bmatrix} \dot{x}_p \\ \dot{y}_p \end{bmatrix} = \begin{bmatrix} K_{vx}\dot{e}_{vx} \\ K_{vy}\dot{e}_{vy} \end{bmatrix} \tag{25}$$

where $\dot{e}_{vp} = v_{\mathrm{d}p} - \dot{p}$ is the velocity errors and $K_{vp} = 3$ is the velocity control coefficient ($p = x, y$). $v_{\mathrm{d}p}$ is found as Equation (26).

$$\begin{bmatrix} v_{\mathrm{d}x} \\ v_{\mathrm{d}y} \end{bmatrix} = \begin{bmatrix} K_x e_x \\ K_y e_y \end{bmatrix} \tag{26}$$

where $e_p = p_d - p$ is the position errors and $K_p = 1$ is position control coefficient.

Table 1 presents the simulation parameters. We took into account measurement noise as well as external disturbances to demonstrate the practical applicability of DOBC approaches. While we gave commands that change in one direction in Cartesian space for the way-point command case, we gave the following simultaneously changing commands

Table 1. Simulation settings for the second scenario.

Δt	Simulation step size	0.001 sec
T	Flight time	140 sec
σ_p	Variance of positional noise	0.001
σ_v	Variance of velocity noise	0.001
Δt_n	Noise step size	0.1 sec
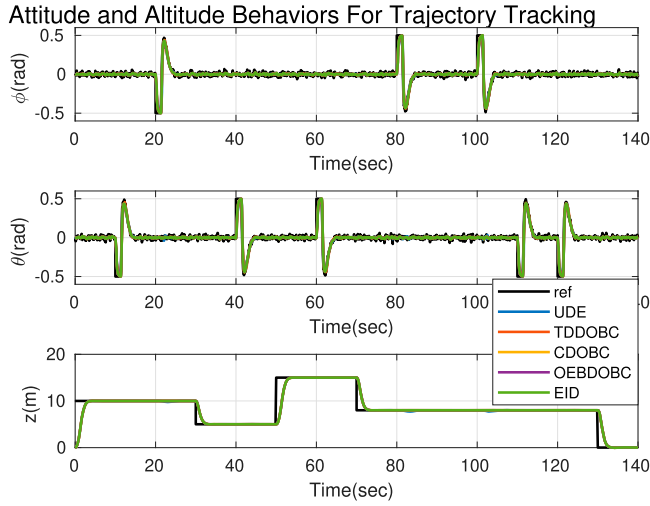
Figure 15. Attitude and altitude behaviors of the quadrotor for way-point tracking.
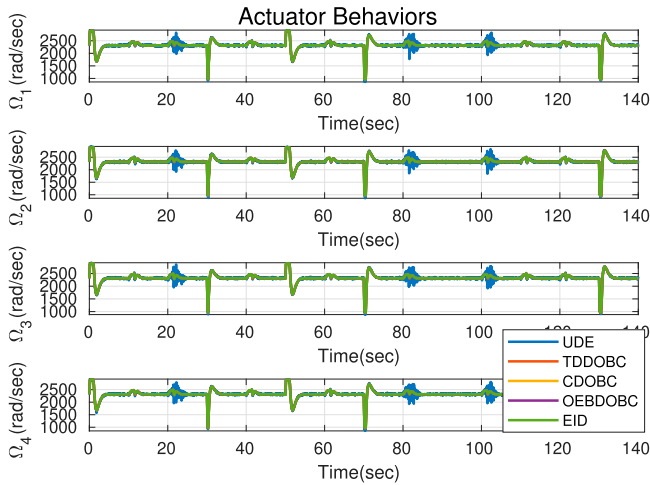
Figure 16. Actuator behaviors of the quadrotor for way-point tracking.

for the trajectory command case.

$$
x_d = \begin{cases}
0 & t < 20 \text{ sec.} \\
\dfrac{t-20}{2} \sin\left(\dfrac{2\pi t}{20}\right) & 20 \le t < 80 \text{ sec.} \\
\dfrac{140-t}{2} \sin\left(\dfrac{2\pi t}{20}\right) & t \ge 80 \text{ sec.}
\end{cases} \tag{27}
$$

Figure 17. Way-point tracking position behaviors of the quadrotor.
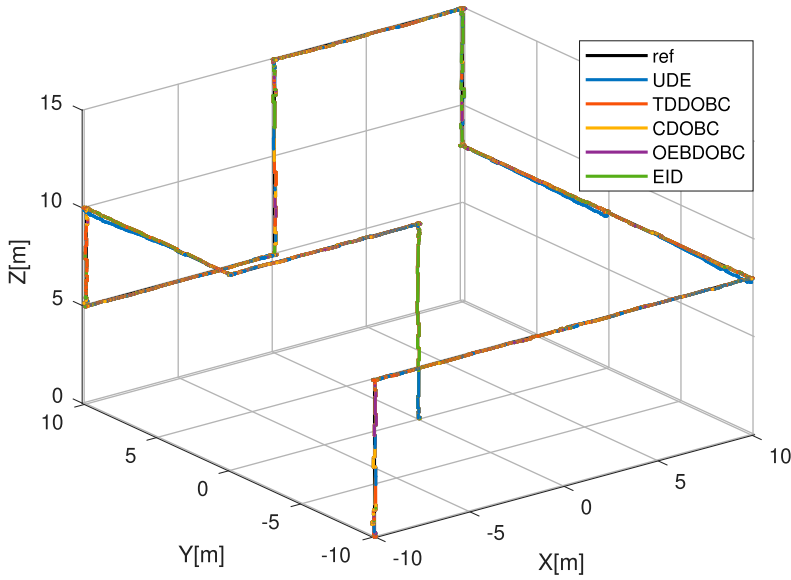
Figure 18. Way-point tracking 3D behaviors of the quadrotor.

$$
y_d = \begin{cases}
0 & t < 20 \text{ sec.} \\
\dfrac{t-20}{2}\cos\left(\dfrac{2\pi t}{20}\right) & 20 \le t < 80 \text{ sec.} \\
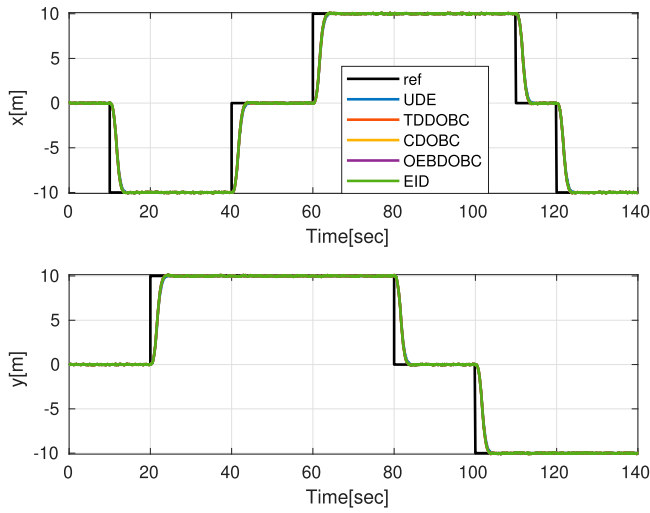\dfrac{140-t}{2}\cos\left(\dfrac{2\pi t}{20}\right) & t \ge 80 \text{ sec.}
\end{cases} \tag{28}
$$

$$
z_d = \begin{cases}
10\tanh\left(\dfrac{t}{5}\right) & t < 20 \text{ sec.} \\
10 & 20 \le t < 80 \text{ sec.} \\
\dfrac{140-t}{6} & t \ge 80 \text{ sec.}
\end{cases} \tag{29}
$$
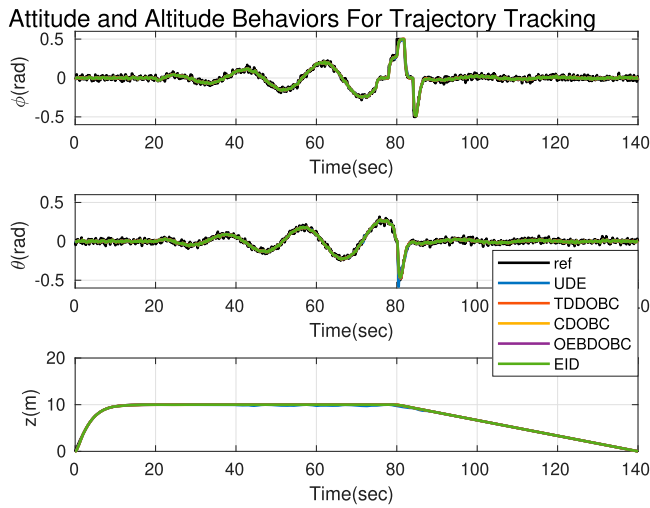
Figure 19. Attitude and altitude behaviors of the quadrotor for trajectory tracking.
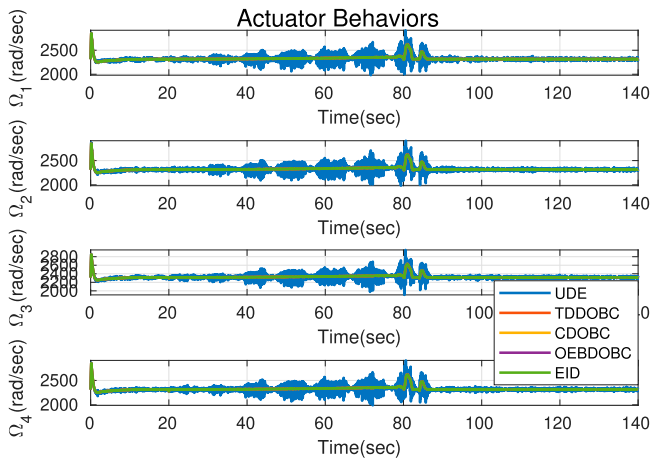
Figure 20. Actuator behaviors of the quadrotor for trajectory tracking.

Figure 15 shows the roll, pitch and altitude behaviors of the quadrotor under the way-point reference commands. Figure 16 depicts the angular speeds of the quadrotor for the same command set. In Figures 17 and 18, translational behaviors of the quadrotor are presented. For the trajectory commands case, Figures 19–22 illustrate the orientational, actuator and trajectory tracking behaviors of the quadrotor. Scenario 2 simulation studies (Figures 16 and 20) have shown that the UDE method is also more sensitive to measurement noise.

BSC scheme failed to follow the both way-point and trajectory reference commands. However, all DOBC approaches have successfully completed the given way-point and trajectory commands. The experiments made proved the practical applicability of these methods, which are successful even under measurement noise.
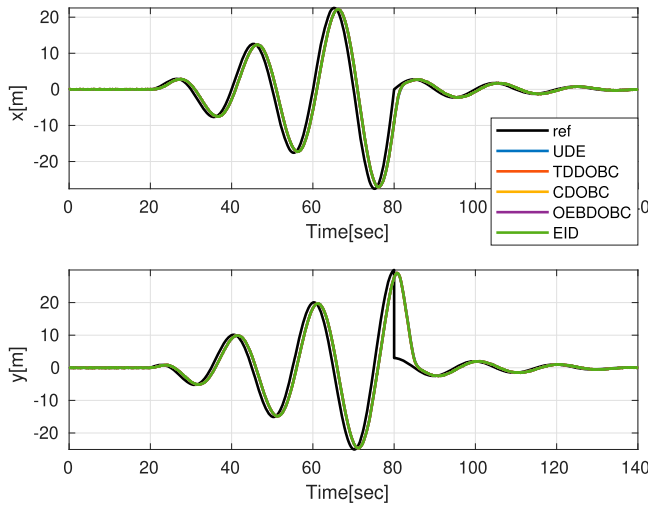
Figure 21. Trajectory tracking position behaviors of the quadrotor.
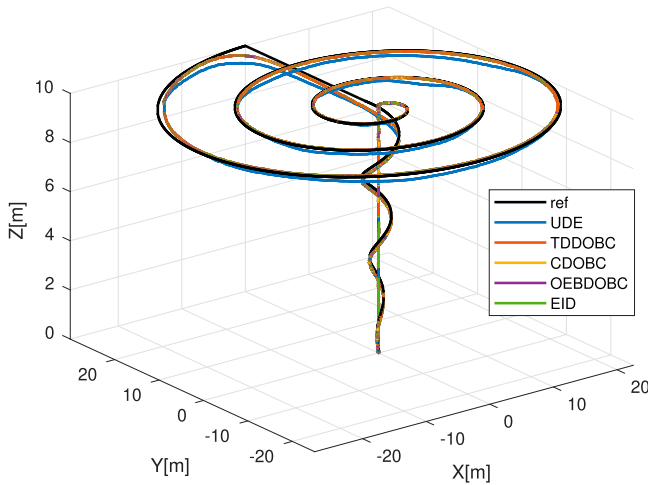
Figure 22. Trajectory tracking 3D behaviors of the quadrotor.

4. Conclusion

In this paper, a short tutorial introduction to DOBC approaches for the quadrotors was presented to obtain robust autopilot architectures. The modeling and controlling of a quadrotor were explained and five different DOBC approaches were adapted in its overall architecture. DOBC design steps were given in detail by design challenges. To show their disturbance rejection capabilities and practical applicability, two flight simulation scenarios were carried out. For all simulation cases, we only took into account the external disturbances in rotational motions. While we gave the attitude trajectory commands to quadrotor attitude control architecture in the first scenario, we issued both way-point and trajectory commands to an outer loop controlling the translational motions in the

second one. Presented DOBC approaches have successfully completed the given reference commands in the presence of the external disturbances even under the measurement noise. Moreover, simulation experiments have shown that UDEBC approach transmits the external disturbance and measurement noise effects to the actuators directly. As a result, for UDEBC approach, it should be kept in mind that flight accidents may occur due to excessive ESC heating. Baseline attitude controller without DOBC approach have failed to follow the given reference commands. The simulation studies have also proved the practical applicability of these methods, which are successful even under measurement noise.

Acknowledgements

Disclosure statement

No potential conflict of interest was reported by the authors.

Notes on contributors

Abdurrahman Bayrak received the B.S. degree from the Department of Electrical and Electronics Engineering, Pamukkale University, Denizli, Turkey, in 2011, the Master's degree from the Department of Computer Engineering, Hacettepe University, Ankara, Turkey, in 2016.

He is currently a Ph.D. student in the Department of Computer Engineering at Hacettepe University, Ankara, Turkey. His scientific research areas includes: Robust Control, Guidance, Navigation and Control, Dynamic System Modelling and Simulation, Unmanned and Autonomous Systems.

Mehmet Önder Efe (M'04, SM'07) received the B.S. degree from the Department of Electronics and Communications Engineering, İstanbul Technical University, İstanbul, Turkey, in 1993, the M.S. degree from the Department of Systems and Control Engineering, Boğaziçi University, İstanbul, Turkey, in 1996, and the Ph.D. degree from the Department of Electrical and Electronics Engineering, Boğaziçi University, in 2000. He is now with the Department of Computer Engineering, Hacettepe University, Ankara, Turkey. Dr. Efe is/was an editor/associate editor of *IEEE Transactions on Artificial Intelligence*, *IEEE Transactions on Industrial Electronics*, *IEEE Transactions on Industrial Informatics*, *IEEE/ASME Transactions on Mechatronics*, *Trans. of the Institute of Measurement and Control, and Measurement & Control*.

ORCID

Abdurrahman Bayrak 🔾 http://orcid.org/0000-0001-6166-7894
Mehmet Önder Efe 🔾 http://orcid.org/0000-0002-5992-895X

References

Alexis, K., G. Nikolakopoulo, and A. Tzes. 2012. "Model Predictive Quadrotor Control: Attitude, Altitude and Position Experimental Studies." *IET Control Theory & Applications* 6 (12): 1812–1827.

Bangura, M., and R. Mahony. 2014. "Real-time Model Predictive Control for Quadrotors." *IFAC Proceedings Volumes* 47 (3): 11773–11780.

Bayrak, A., M. Ö. Efe. 2019. "Disturbance Uncertainty Estimator Based Robust Attitude Control of a Quadrotor." In *10th Ankara International Aerospace Conference.*

Bayrak, A., M. Ö. Efe. 2021. "A Frequency Domain Comparison of Disturbance Observer Based Control Schemes." *Proceedings of the Institution of Mechanical Engineers, Part I: Journal of Systems and Control Engineering* 23509596518211036597.

Bouabdallah, S. 2007. "Design and Control of Quadrotors With Application to Autonomous Flying." *Epfl*, no. Thesis.

Bouabdallah, S., A. Noth, and R. Siegwart. 2004. "PID Vs LQ Control Techniques Applied to An Indoor Micro Quadrotor." *IEEE/RSJ International Conference on Intelligent Robots and Systems* 3: 2451–2456.

Bouabdallah, S., and R. Siegwart. 2005. "Backstepping and Sliding-Mode Techniques Applied to an Indoor Micro Quadrotor." In *IEEE International Conference on Robotics and Automation*, 2247–2252.

Bouabdallah, S., and R. Siegwart. 2007. "Full Control of a Quadrotor." In *IEEE/RSJ International Conference on Intelligent Robots and Systems*, 153–158.

Cai, W., J. She, M. Wu, and Y. Ohyama. 2019. "Disturbance Suppression for Quadrotor UAV Using Sliding-mode-observer-based Equivalent-input-disturbance Approach." *ISA Transactions* 92: 286–297.

Castillo, A., R. Sanz, P. Garcia, W. Qiu, H. Wang, and C. Xu. 2019. "Disturbance Observer-based Quadrotor Attitude Tracking Control for Aggressive Maneuvers." *Control Engineering Practice* 82: 14–23.

Chen, F., R. Jiang, K. Zhang, B. Jiang, and G. Tao. 2016. "Robust Backstepping Sliding-mode Control and Observer-based Fault Estimation for a Quadrotor UAV." *IEEE Transactions on Industrial Electronics* 63 (8): 5044–5056.

Chen, W., J. Yang, L. Guo, and S. Li. 2016. "Disturbance-Observer-Based Control and Related Methods – An Overview." *IEEE Transactions on Industrial Electronics* 63 (2): 1083–1095.

Förster, J. 2015. "System Identification of the Crazyflie 2.0 Nano Quadrocopter." Bachelor's Thesis, ETH Zurich.

Invernizzi, D., P. Panizza, F. Riccardi, S. Formentin, and M. Lovera. 2016. "Data-driven Attitude Control Law of a Variable-pitch Quadrotor: a Comparison Study." *IFAC-PapersOnLine* 49 (17): 236–241.

Khatoon, S., M. Shahid, and H. Chaudhary. 2014. "Dynamic Modeling and Stabilization of Quadrotor Using PID Controller." In *International Conference on Advances in Computing, Communications and Informatics (ICACCI)*, 746–750.

Kürkçü, B., C. Kasnakoğlu, and M. Ö. Efe. 2018. "Disturbance/uncertainty Estimator Based Integral Sliding-mode Control." *IEEE Transactions on Automatic Control* 63 (11): 3940–3947.

Lazim, I. M., A. R. Husain, Z. Mohamed, M. A. M. Basri, N. A. M. Subha, and L. Ramli. 2019. "Disturbance Observer-based Formation Tracking Control of Multiple Quadrotors in the Presence of Disturbance." *Transactions of the Institute of Measurement and Control* 41 (14): 4129–4141.

Lu, Q., B. Ren, S. Parameswaran, and Q. C. Zhong. 2018. "Uncertainty and Disturbance Estimator-based Robust Trajectory Tracking Control for a Quadrotor in a Global Positioning System-denied Environment." *Journal of Dynamic Systems, Measurement, and Control* 140 (3): 031001.

Madani, T., and A. Benallegue. 2006. "Backstepping Control for a Quadrotor Helicopter." In *IEEE/RSJ International Conference on Intelligent Robots and Systems*, 3255–3260.

Nascimento, T. P., and M. Saska. 2019. "Position and Attitude Control of Multi-rotor Aerial Vehicles: A Survey." *Annual Reviews in Control* 48: 129–146.

Ortiz, J. P., L. I. Minchala, and M. J. Reinoso. 2016. "Nonlinear Robust H-Infinity PID Controller for the Multivariable System Quadrotor." *IEEE Latin America Transactions* 14 (3): 1176–1183.

Reyes-Valeria, E., R. Enriquez-Caldera, S. Camacho-Lara, and J. Guichard. 2013. "LQR Control for a Quadrotor Using Unit Quaternions: Modeling and Simulation." In *23rd International Conference on Electronics, Communications and Computing*, 172–178.

Rinaldi, F., S. Chiesa, and F. Quagliotti. 2014. "Linear Quadratic Control for Quadrotors UAVs Dynamics and Formation Flight." *Journal of Intelligent & Robotic Systems* 70 (1-4): 203–220.

Salih, A. L., M. Moghavvemi, H. A. Mohamed, and K. S. Gaeid. 2010. "Flight PID Controller Design for a UAV Quadrotor." *Scientific Research and Essays* 5 (23): 3660–3667.

Sanz, R., P. Garcia, Q. C. Zhong, and P. Albertos. 2016a. "Robust Control of Quadrotors Based on An Uncertainty and Disturbance Estimator." *Journal of Dynamic Systems, Measurement, and Control* 138 (7): 071006-1–071006-8.

Sanz, R., P. Garcia, Q. C. Zhong, and P. Albertos. 2016b. "Predictor-based Control of a Class of Time-delay Systems and Its Application to Quadrotors." *IEEE Transactions on Industrial Electronics* 64 (1): 459–469.

Shaik, M. K., and J. F. Whidborne. 2016. "Robust Sliding Mode Control of a Quadrotor." In *11th International Conference on Control (CONTROL)*, 1–6.

She, J. H., M. X. Fang, Y. Ohyama, H. Hashimoto, and M. Wu. 2008. "Improving Disturbance-Rejection Performance Based on An Equivalent Input-disturbance Approach." *IEEE Transactions on Industrial Electronics (1982)* 55 (1): 380–389.

She, J. H., X. Xin, and Y. D. Pan. 2011. "Equivalent-input-disturbance Approach-Analysis and Application to Disturbance Rejection in Dual-stage Feed Drive Control System." *IEEE/ASME Transactions Mechatronics* 16 (2): 330–340.

Shi, X. N., Y. A. Zhang, and D. Zhou. 2015. "A Geometric Approach for Quadrotor Trajectory Tracking Control." *International Journal of Control* 88 (11): 2217–2227.

Tamaki, K., K. Ohishi, K. Ohnishi, and K. Miyachi. 1986. "Microprocessor-based Robust Control of a DC Servo Motor." *IEEE Control Syst Mag* 6 (5): 30–36.

Treesatayapun, C., and A. J. Munoz-Vazquez. 2021. "Discrete-time Data-driven Disturbance-observer Control." *Journal of Computational Science* 54: 101426.

Wang, H., and M. Chen. 2016. "Trajectory Tracking Control for An Indoor Quadrotor UAV Based on the Disturbance Observer." *Transactions of the Institute of Measurement and Control* 38 (6): 675–692.

Yang, J., W. H. Chen, and S. H. Li. 2010. "Autopilot Design of Bank-to-Turn Missile Using State-Space Disturbance Observers." In *UKACC International Conference on Control*, 1218–1223.

Zhang, Y., Z. Chen, X. Zhang, Q. Sun, and M. Sun. 2018. "A Novel Control Scheme for Quadrotor UAV Based Upon Active Disturbance Rejection Control." *Aerospace Science and Technology* 79: 601–609.

Zhong, Q. C., A. Kuperman, and R. K. Stobart. 2011. "Design of UDE- Based Controllers From Their Two-degree-of-freedom Nature." *International Journal of Robust Nonlinear Control* 17 (21): 1994–2008.

Zhong, Q. C., and D. Rees. 2004. "Control of Uncertain LTI Systems Based on An Uncertainty and Disturbance Estimator." *he Journal of Dynamic Systems, Measurement, and Control* 126 (4): 905–910.

Zulu, A., and S. John. 2016. "A Review of Control Algorithms for Autonomous Quadrotors." *arXiv preprint arXiv:1602.02622*.

Appendices

Appendix 1. Physical parameters of the quadrotor model

We chose the Crazyflie 2.0 nanoquadrotor platform to show the effectiveness of the control schemes presented in this paper. The Crazyflie 2.0 nanoquadrotor platform parameters are given in Table A1 (Förster 2015).

Appendix 2. Baseline Controller Parameters

Table A2 shows the BS controller parameters presented in section "Baseline Controller Design". These parameters were found by trial and error such that the settling time is less than 1 second for attitude control, 3 seconds for altitude control and no overshoot. It should be noted here that we do

Table A1. Physical parameters of the Crazyflie 2.0 nanoquadrotor.

Symbol	Value (unit)
m	0.028 (kg)
l	0.065 (m)
K_F	1.61×10^{-8} (N.s^2)
κ	0.006
I_x	16.571710×10^{-6} (kg.m^2)
I_y	16.655602×10^{-6} (kg.m^2)
I_z	29.261652×10^{-6} (kg.m^2)
g	9.8 (m/s^2)
J	0
T_{rot}	0.05
Ω_{max}	3050 (rad/sec)
Ω_{min}	0 (rad/sec)
$U_{1\,max}$	0.71 (N)
$U_{1\,min}$	0.07 (N)
τ_{max}	1×10^{-3} (Nm)
τ_{min}	-1×10^{-3} (Nm)

Table A2. BSC approach parameters.

	z	ϕ	θ	ψ
α_{*1}	2	6	6	6
α_{*2}	1	6	6	6

not concentrate on finding the most appropriate parameters for baseline controller preferred as it will affect the tracking performance rather than the robustness of the system, regardless of the way the parameters are found.

Appendix 3. CDOBC Approach Parameters

Table A3 illustrates the parameters required for the LPF design proposed by us in the section "CDOBC Scheme".

Table A3. CDOBC approach LPF design parameters.

K_p	K_d
0.2	0.005

Appendix 4. OEBDOBC Approach Parameters

The following equation is the output of "**K_obs**" block for each rotational movement of a quadrotor.

$$\hat{d}_i = K_{pi}\varepsilon_i + K_{di}\dot{\varepsilon}_i \tag{A1}$$

where $i \in (\phi, \theta, \psi)$.

Observer parameters required for the design of "$\mathbf{K_{obs}}$" block are given in Table A4.

Table A4. OEBDOBC approach observer parameters.

	z	ϕ	θ	ψ
K_{p*}	0	0.2	0.2	0.2
K_{d*}	0	0.005	0.005	0.005

Appendix 5. EIDBC Approach Parameters

The following equations show the system matrix, control matrix and output matrix of quadrotor nominal plant for each rotational motion.

$$\mathbf{A_{n\phi}} = \begin{bmatrix} 0 & 0 \\ 1 & 0 \end{bmatrix} \mathbf{B_{n\phi}} = \begin{bmatrix} 1 \\ 0 \end{bmatrix} \mathbf{C_{n\phi}} = \begin{bmatrix} 0 & 60344 \end{bmatrix} \tag{A2}$$

$$\mathbf{A_{n\theta}} = \begin{bmatrix} 0 & 0 \\ 1 & 0 \end{bmatrix} \mathbf{B_{n\theta}} = \begin{bmatrix} 1 \\ 0 \end{bmatrix} \mathbf{C_{n\theta}} = \begin{bmatrix} 0 & 60040 \end{bmatrix} \tag{A3}$$

$$\mathbf{A_{n\psi}} = \begin{bmatrix} 0 & 0 \\ 1 & 0 \end{bmatrix} \mathbf{B_{n\psi}} = \begin{bmatrix} 1 \\ 0 \end{bmatrix} \mathbf{C_{n\psi}} = \begin{bmatrix} 0 & 34174 \end{bmatrix} \tag{A4}$$

We give the EIDBC approach observer gain parameters in Table A5. These parameters were found by the Ackermann method. Moreover, for LPF "$\mathbf{F(s)}$" block, we set T_e cutoff frequency in Equation 15 as 100 rad/sec.

Table A5. EIDBC approach observer gain parameters.

	ϕ	θ	ψ
$\mathbf{L}_i$	$[0.4972\ 0.0058]^T$	$[0.4997\ 0.0058]^T$	$[0.8778\ 0.0102]^T$

Appendix 6. TDDOBC approach parameters

The following equations show the system matrix, control matrix and output matrix of quadrotor nominal plant for each rotational motion.

$$\mathbf{A_{n\phi}} = \begin{bmatrix} 0 & 0 \\ 1 & 0 \end{bmatrix} \mathbf{B_{n\phi}} = \begin{bmatrix} 60344 \\ 0 \end{bmatrix} \mathbf{C_{n\phi}} = \begin{bmatrix} 0 & 1 \end{bmatrix} \tag{A5}$$

$$\mathbf{A_{n\theta}} = \begin{bmatrix} 0 & 0 \\ 1 & 0 \end{bmatrix} \mathbf{B_{n\theta}} = \begin{bmatrix} 60040 \\ 0 \end{bmatrix} \mathbf{C_{n\theta}} = \begin{bmatrix} 0 & 1 \end{bmatrix} \tag{A6}$$

$$\mathbf{A_{n\psi}} = \begin{bmatrix} 0 & 0 \\ 1 & 0 \end{bmatrix}, \mathbf{B_{n\psi}} = \begin{bmatrix} 34174 \\ 0 \end{bmatrix}, \mathbf{C_{n\psi}} = \begin{bmatrix} 0 & 1 \end{bmatrix} \tag{A7}$$

Table A6 presents the observer gain parameters found by the Ackermann method.

Table A6. TDDOBC approach observer gain parameters.

	ϕ	θ	ψ
$\mathbf{L}_i$	$[0.008\ 0.003]$	$[0.008\ 0.003]$	$[0.008\ 0.003]$

Appendix 7. UDEBC Approach Parameters

UDEBC approach controller parameters in Equation (19) are given in Table A7. The UDE controller parameters were selected by following the parameter finding steps in the reference study of Lu et al. (2018).

Table A7. UDEBC approach parameters.

	ϕ	θ	ψ
K_i	4	4	4
T_i	0.001	0.001	0.001
λ_i	2	2	2